

The Effects of Undulator Field on Stored Electron Beam

Thananchai DASRI¹ and Supagorn RUGMAI^{2,3}

¹School of Science and Technology, Nong Khai Campus, Khon Kaen University, Nong Khai 43000, Thailand

²School of Physics, Suranaree University of Technology, Nakhon Ratchasima 30000, Thailand

³Synchrotron Light Research Institute, Nakhon Ratchasima 30000, Thailand

(Corresponding author; e-mail: thananchai_dasri@hotmail.com)

Received: 5 September 2011, Revised: 5 December 2011, Accepted: 29 December 2011

Abstract

In order to extend the usable photon spectrum to higher photon flux, an undulator with periodic magnetic field has to be installed into the storage ring of the synchrotron facility. This paper presents the perturbations from the magnetic field of such a device on the electron beam dynamics in the ring. Theories and an example of a practical device are discussed. The U60 undulator of the Siam Photon Source is selected for illustrating these ideas.

Keywords: Synchrotron radiation, perturbation, undulator, storage ring

Introduction

Synchrotron radiation (SR) is the electromagnetic radiation emitted when charged relativistic particles are transversally accelerated. The most common synchrotron light source is a bending magnet installed in the storage ring of a synchrotron facility. However, various experiments require higher quality synchrotron light, shown in **Figure 1**. An undulator is another type of the device for fulfilling this requirement. The U60 undulator at the Siam Photon Source (SPS) has been illustrated in a previous paper [1]. Generally, when an electron moves in the storage ring the position and angle of the electrons will be forced into the designed orbit, shown in **Figure 2**. If the position and angle of electrons at any point in a storage ring are mapped into the phase space (x, x') , the phase space ellipse with an area of $\pi\varepsilon$ is obtained, as shown in **Figure 2**. The equation of the ellipse at any given location s , can be written as,

$$x(s)^2 + \left(\frac{2\alpha_s x'(s)}{\gamma_s}\right)x'(s) + \left(\frac{\beta_s x'(s)^2 - \varepsilon}{\gamma_s}\right) = 0 \quad (1)$$

The ellipse shape changes along the beam path s . This ellipse is related to the twiss parameters: β , α and γ . These parameters are related to the maximum amplitude and angle of the oscillation, at a given location s :

$$x_{\max}(s), y_{\max}(s) = \sqrt{\varepsilon_{x,y}(s)\beta_{x,y}(s)}, \quad (2)$$

$$x'_{\max}(s), y'_{\max}(s) = \sqrt{\frac{\varepsilon_{x,y}(s)}{\beta_{x,y}(s)}}. \quad (3)$$

The twiss parameters are periodic functions of s . They completely describe the properties of the magnetic lattice of the storage ring. For example, the SPS storage ring twiss parameters calculated using the Accelerator Toolbox (AT) [2] are shown in the **Figures 4, 5** and **6**. **Figure 7** shows the dispersion functions (η_x and η_y) of the SPS storage ring. The dispersion function is introduced as a result of the fact that the energy of the electrons differ from the nominal energy.

However, when the undulator is inserted in the stored ring, the position, angle of electrons and twiss parameters will be changed. The purpose of this paper is to present the effects of the undulator

linear field, dipole and quadrupole field components, on the electron beam in the storage ring.

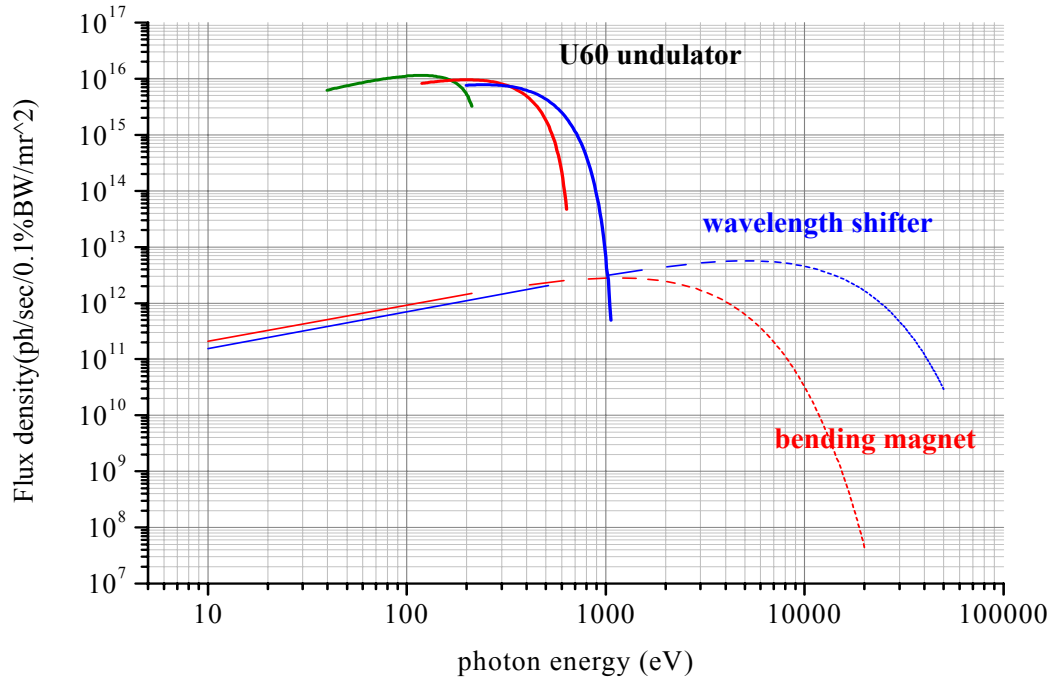


Figure 1 Flux density as a function of photon energy, up to the 5th harmonic, emitted by a 1.2 GeV electron beam of 100 mA through the U60 undulator, compared with a bending magnet and wavelength shifter spectrum.

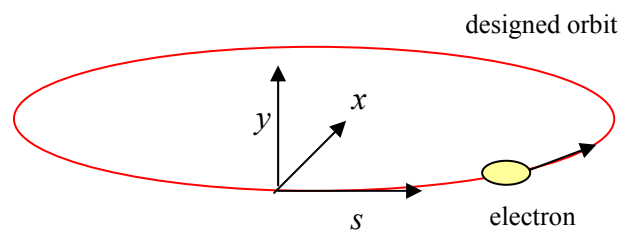


Figure 2 Electron is forced to move in an ideal orbit.

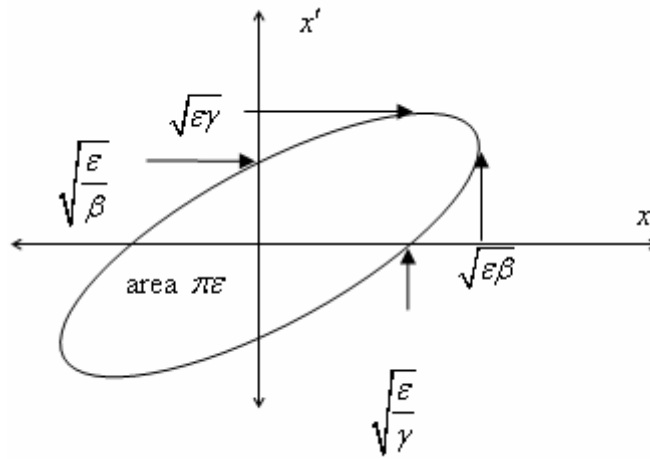


Figure 3 Phase space ellipse.

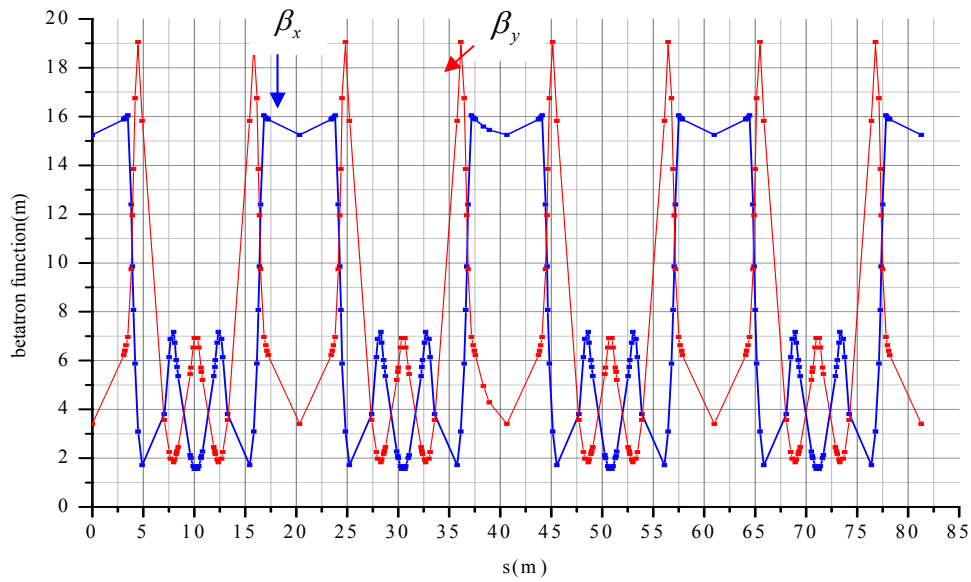


Figure 4 β function of the SPS storage ring.

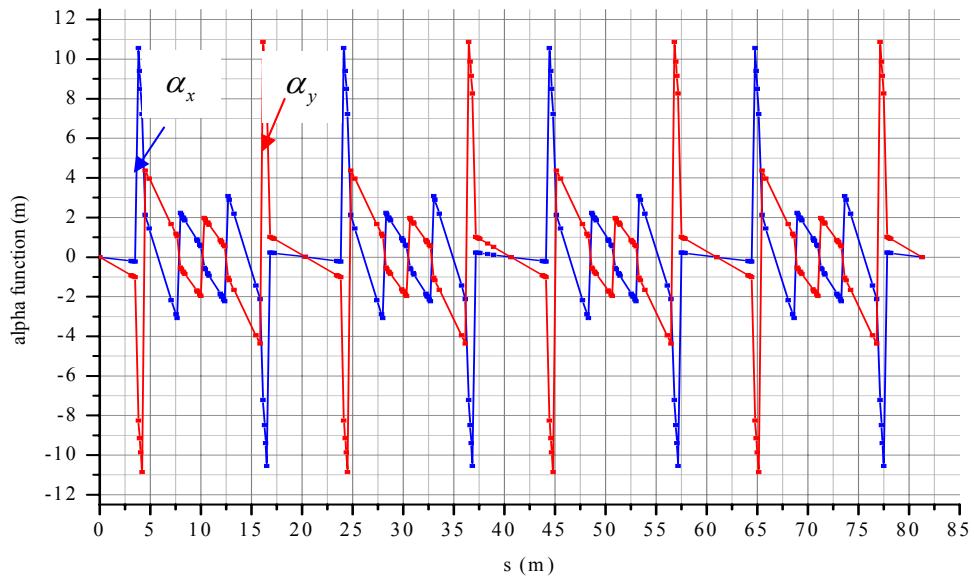


Figure 5 α function of the SPS storage ring.

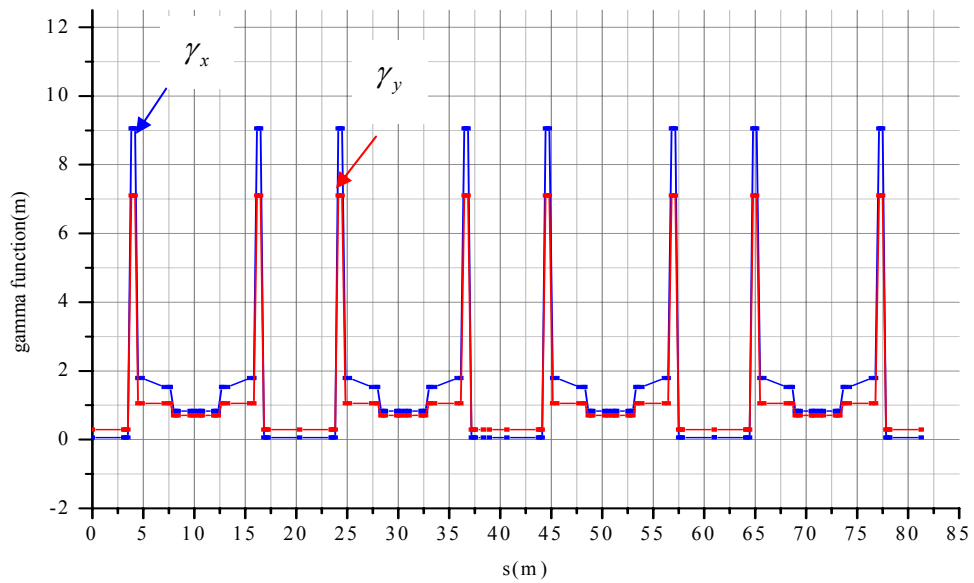


Figure 6 γ function of the SPS storage ring.

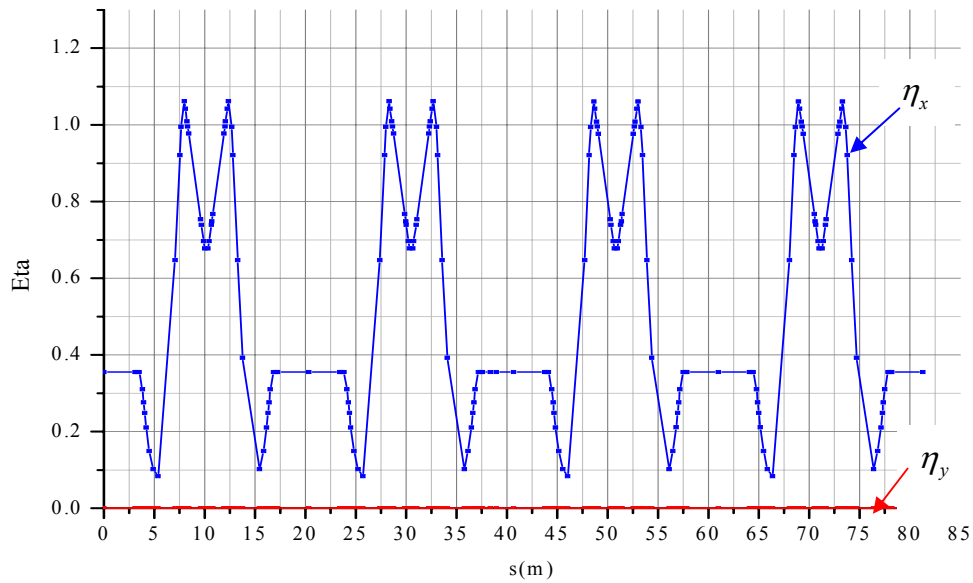


Figure 7 The dispersion function of the SPS storage ring.

Methods, results and discussion

Effects of the dipole field component

The dipole field component of the undulator produces a transverse displacement of the electron with a sinusoidal-like trajectory. The electron motion is explained by the Lorentz force equation:

$$\gamma m_o \frac{d^2 \vec{r}}{dt^2} = q(\vec{v} \times \vec{B})$$

For the vertical magnetic field component $B_y(z)$, by making the integration along the longitudinal coordinate the horizontal electron angle is obtained:

$$x'(z) = \frac{0.3}{E[GeV]} I_y(z) \tag{4}$$

where $I_y(z)$ is the vertical first field integral, given by

$$I_y(z) = \int_{z'=0}^{z'=z} B_y(z') dz' \tag{5}$$

By making the integration of the electron angle in Eq. (4), the electron trajectory can be calculated by

$$x(z) = \frac{0.3}{E[GeV]} II_y(z) \tag{6}$$

where $II_y(z)$ is the vertical second field integral given by

$$II_y(z) = \int_{z'=0}^{z'=z} \int_{z''=0}^{z''=z'} B_y(z'') dz'' dz' \tag{7}$$

By assigning an upper limit of the integration $z' = L$ and the undulator's magnetic length in Eq. (4) and Eq. (6), the angle of deviation and transverse positions of the electron at the exit of the undulator can be respectively evaluated as

$$\Delta x' = x'(z' = L) \tag{8}$$

and

$$\Delta x = x(z = L) \tag{9}$$

Figure 8 illustrates the effects of the dipole field on the electron beam. Consequently, the closed orbit distortion (COD) can be predicted in the beam position monitors (BPM) numbered j by using the obtained deviated electron angle at the exit of the undulator

$$\Delta = \frac{\theta \sqrt{\beta_i \beta_j}}{2 \sin \pi \nu} \cos(|\mu_i - \mu_j| - \nu \pi) \tag{10}$$

Where $\theta = \Delta x'$ is the kicked electron angle, μ is the phase advance and ν is the betatron tune. Subscripts i and j indicate the positions at the exit

of an undulator and BPMs. The measured field of U60 undulator is exemplified in **Figure 9** [3]. The horizontal deflection angle and electron trajectory can then be integrated. The results are shown in **Figures 10 and 11**, respectively. The results show

that the electron beam exits the undulator with a finite angle and position. The maximum angle is 0.197 mrad and the transverse position is 324.1 μm at the undulator gap of 26.5 mm.

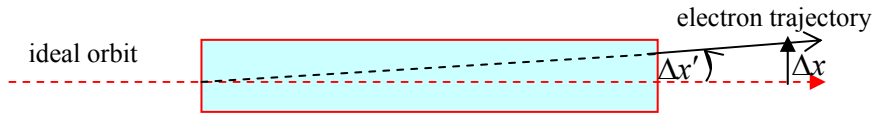


Figure 8 The effects of undulator dipole field on an electron.

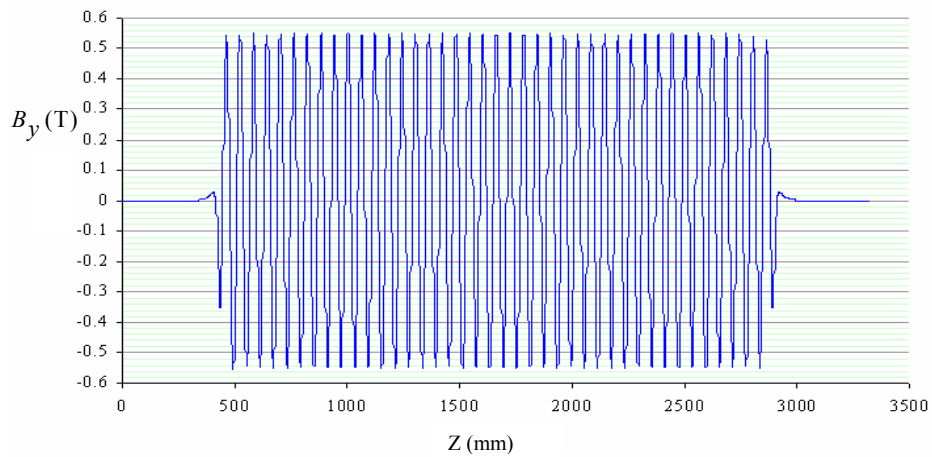


Figure 9 Undulator magnetic field at a gap of 26.5 mm.

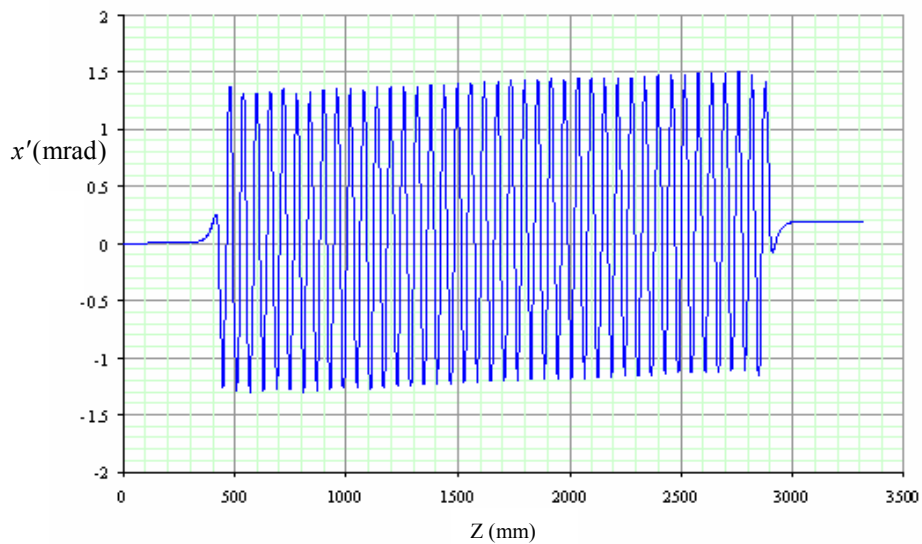


Figure 10 Electron angles at a gap of 26.5 mm.

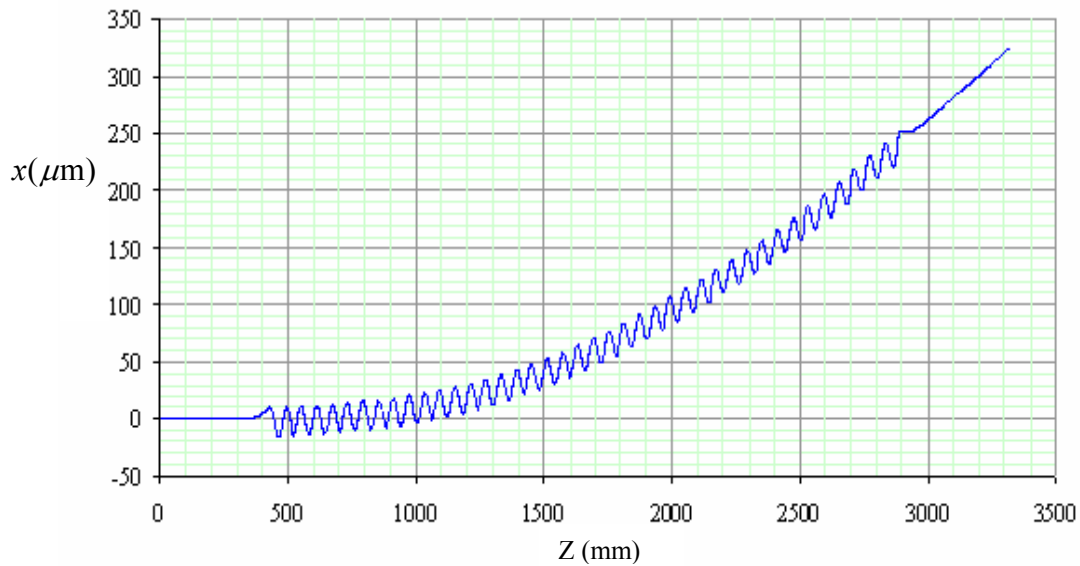


Figure 11 Electron trajectories at a gap of 26.5 mm.

Effects of the quadrupole field component

Insertion of the undulator into the storage ring causes betatron tune shifts. The betatron tune shifts are calculated using Matlab programming with the Accelerator Toolbox [2]. The tune shifts can be calculated by a linear perturbation method [4-6]. The vertical focusing strength of the undulator and the phase advance are evaluated from Eq. (11) and Eq. (12), respectively.

$$K_y = \left(\frac{0.3}{E(\text{GeV})} \right)^2 \frac{1}{L} \int_0^L B_y^2(z) dz \quad (11)$$

$$\mu_y = \cos^{-1} \left(\frac{1}{2} \text{Tr}(M_C M_{F,\text{eff}}) \right) \quad (12)$$

The vertical tune shift can be eventually calculated by

$$\Delta \nu_y = \frac{\mu_u - \mu_y}{2\pi} \quad (13)$$

where M_C is the one turn matrix without an undulator:

$$M_C = \begin{pmatrix} \cos \mu_y + \alpha_y \sin \mu_y & \beta_y \sin \mu_y \\ -\gamma_y \sin \mu_y & \cos \mu_y - \alpha_y \sin \mu_y \end{pmatrix},$$

$M_{F,\text{eff}}$ is defined by

$$M_{F,\text{eff}} = \begin{pmatrix} 1 & -\frac{L}{2} \\ 0 & 1 \end{pmatrix} \begin{pmatrix} \cos \sqrt{K_y L} & \frac{1}{\sqrt{K_y}} \sin \sqrt{K_y L} \\ -\sqrt{K_y} \sin \sqrt{K_y L} & \cos \sqrt{K_y L} \end{pmatrix} \begin{pmatrix} 1 & -\frac{L}{2} \\ 0 & 1 \end{pmatrix}$$

$M_C M_{F,\text{eff}}$ is therefore the one turn matrix in presence of the undulator given by

$$M_C M_{F,\text{eff}} = \begin{pmatrix} \cos \mu_u + \alpha_y \sin \mu_u & \beta_u \sin \mu_u \\ -\gamma_u \sin \mu_u & \cos \mu_u - \alpha_u \sin \mu_u \end{pmatrix} \quad (14)$$

The analytical calculation gives a larger vertical tune shift, with a value of 0.0064 at the minimum gap.

Tune shift presenting above are only produced from the intrinsic focusing of the undulator magnet. However, the tune shift is also produced from undulator field errors. Effects from the field error alone can be evaluated by performing polynomial fits on the measured field integrals along the horizontal position [3]. The multipole expansion of the field integrals are obtained by

$$I_i(x) = \int_{z'=0}^L B_i(z')dz = B_{0,i}L + (B'_iL)x + \left(\frac{1}{2}B''_iL\right)x^2 + \dots$$

or

$$I_i(x) = a + bx + cx^2 + \dots \tag{15}$$

where L is the length of the long coil, $a = B_{0,i}L$, $b = B'_iL$ and $c = \frac{B''_iL}{2}$ are the dipole, quadrupole and sextupole components, respectively. Subscript i is a component x or y . For the vertical field component, the quadrupole strength due to undulator field errors is therefore given by

$$K_y[m^{-2}] = \frac{b}{B\rho} \tag{16}$$

where $B\rho = \frac{E[\text{GeV}]}{0.29979}$ is the magnetic rigidity, ρ is the bending radius. For the SPS the electron energy E is 1.2 GeV. By substituting quadrupole strength in the undulator matrix $M_{F,eff}$, the tune shift due to the quadrupole component can be calculated. Therefore, the summation of vertical tune shifts due to intrinsic field using the analytical calculation and field error obtained, are shown in **Figure 12**. The result shows that larger vertical tune shift at a minimum gap is 0.0066 [3]. The result from the experiment, by operating the SPS synchrotron after installing the U60 undulator, at the same gap is 0.0065 [3].

Eventually, the theoretical betatron functions calculated before and after inserting the U60 undulator in the SPS storage ring, using AT [2], obtained are shown in **Figure 13**. The graph in **Figure 13b** is the result at a minimum gap of 26.5 mm. The figures show that the resulting perturbations with the undulator are found to be small, compared with the results without this device.

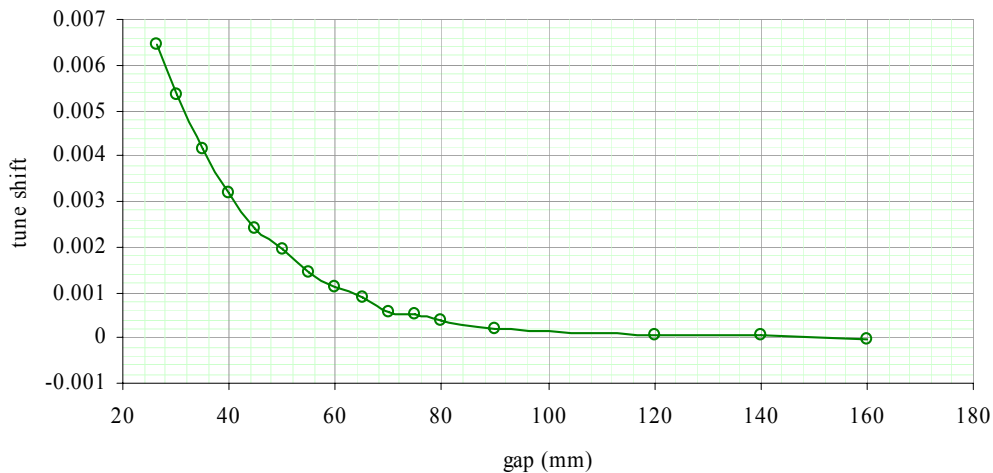
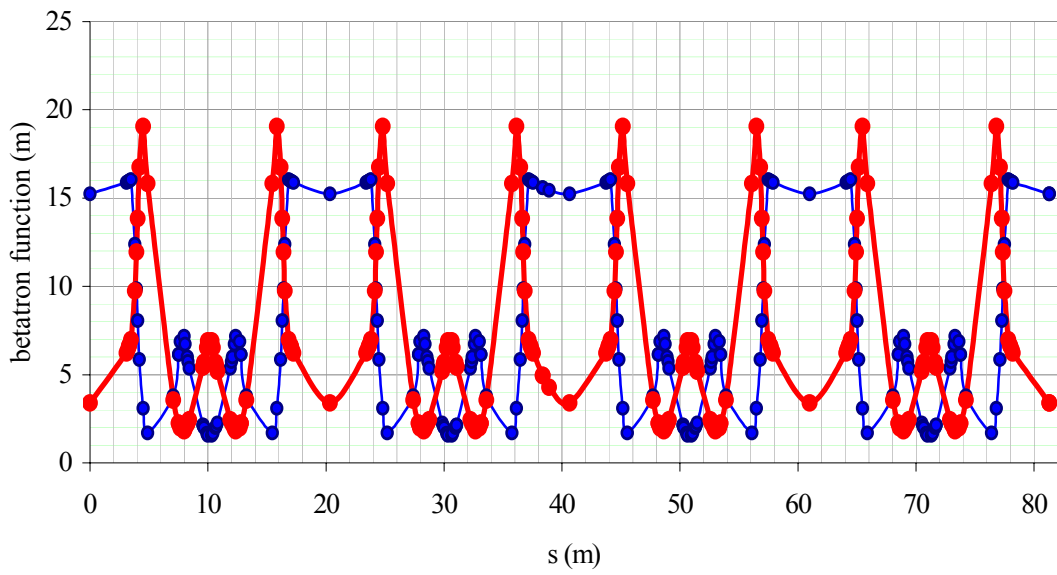
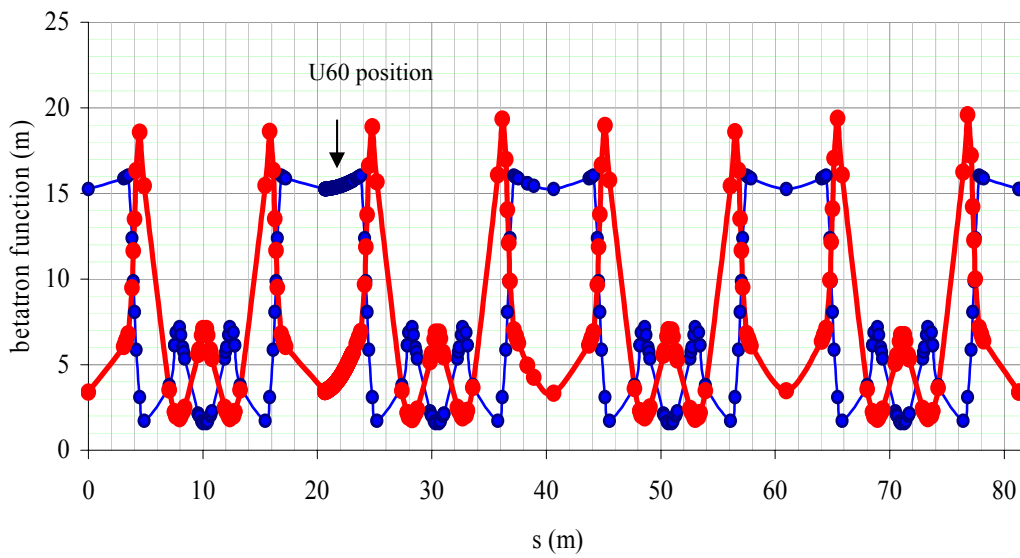


Figure 12 The vertical tune shift due to the U60 undulator that is the summation of intrinsic field and field error.



(a)



(b)

Figure 13 The betatron function of (a) without undulator, (b) with the undulator at a minimum gap of 26.5 mm. The thin lines are β_x and thick lines are β_y .

Summary

Although the installing an undulator in the ring will improve the photon flux, it also perturbs the stored electron beam. The degree of perturbation by a real device is presented. The U60 undulator of the Siam Photon Source is selected as a real device. The dipole field perturbs the angle and position of a stored electron beam. The electron beam exits the device with a non-zero angle and position. The quadrupole field perturbs the betatron function and shifts the electron tune. Betatron and tune shifts resulting from perturbation of the undulator are also found to be small. These effects are found to be significant but may be compensated for after operating the device.

Acknowledgements

The author is grateful to Asst. Prof. Dr. Supagorn Rugmai, his Ph.D. thesis advisor for his valuable advice, kindness, and suggestions about the basic theory of insertion devices and synchrotron light sources.

References

- [1] T Dasri. U60 Undulator: An insertion device for the Siam Photon Source. *Walailak J. Sci. & Tech.* 2011; **8**, 1-8.
- [2] A Terebilo. Accelerator Toolbox for MATLAB. *SLAC-PUB-8732*. 2001.
- [3] T Dasri. 2008, Characterization of Soft X-ray Undulator for the Siam Photon Source, Ph. D. Dissertation. Suranaree University of Technology, Nakhon Ratchasima, Thailand.
- [4] S Rugmai. Effects of high field permanent magnet insertion device on the Siam photon source storage ring. *ScienceAsia*. 2005; **31**, 159-65.
- [5] RP Walker. Wigglers. *In: Proceeding of the CERN Accelerator School Proceeding*. 1995, 807-35.
- [6] M Bassetti, A Cattoni, A Luccio, M Preger, and S Tazzari. *A Transverse Wiggler Magnet for ADONE*. *In: Laboratori Nazionali Frascati Technical Notes LNF-77/26(R)*. 1977.